NMR assignments and secondary structure of the UvrC binding domain of UvrB

Alexander Alexandrovich[a], Mark R. Sanderson[a], Geri F. Moolenaar[b], Nora Goosen[b], Andrew N. Lane[c,*]

[a] *The Randall Institute, King's College, 26-29 Drury Lane, London WC2B 5RL, UK*
[b] *Laboratory of Molecular Genetics, Gorlaeus Laboratories, Einsteinweg 55, Leiden University, Postbus 9502, 2300 RA Leiden, The Netherlands*
[c] *Division of Molecular Structure, National Institute for Medical Research, The Ridgeway, Mill Hill, London NW7 1AA, UK*

Received 5 March 1999; received in revised form 8 April 1999

Abstract The 55 residue C-terminal domain of UvrB that interacts with UvrC during excision repair in *Escherichia coli* has been expressed and purified as a $(His)_6$ fusion construct. The fragment forms a stable folded domain in solution. Heteronuclear NMR experiments were used to obtain extensive ^{15}N, ^{13}C and ^{1}H NMR assignments. NOESY and chemical shift data showed that the protein comprises two helices from residues 630 to 648 and from 652 to 670. ^{15}N relaxation data also show that the first 11 and last three residues are unstructured. The effective rotational correlation time within the structured region is not consistent with a monomer. This oligomerisation may be relevant to the mode of dimerisation of UvrB with the homologous domain of UvrC.

Key words: UvrB protein; UvrC binding; NMR; Protein structure

1. Introduction

Nucleotide excision repair of damaged DNA is achieved in *Escherichia coli* by a complex mechanism, involving the sequential action of six proteins. The UvrA and UvrB proteins form a hetero-oligomer $UvrA_2B$ that recognises and binds to DNA at the site of the lesion. Next, concomitant with ATP hydrolysis, conformational changes occur in the $UvrA_2B$-DNA complex resulting in the tight binding of UvrB and the release of UvrA. This UvrB-DNA pre-incision complex is subsequently bound by UvrC and a nick is made at the fourth or fifth phosphodiester bond 3′ to the lesion. This nick is immediately followed by a second nick at the eighth phosphodiester bond 5′ to the lesion. The 12–13-mer oligonucleotide containing the lesion is removed by the action of UvrD (helicase II), the resulting gap is filled in by DNA polymerase I and finally, the remaining nick is sealed by DNA ligase [1,2].

The domain of UvrB that binds to UvrC was mapped in the C-terminal moiety of the protein [3]. This domain, which is predicted to be helical, interacts with a region of UvrC that is homologous to the UvrB domain, suggesting that the dimerisation occurs through a structurally homologous feature, such as a coiled-coil interaction [3,4].

To provide insight into the dimerisation mechanism between UvrB and UvrC, we have cloned and expressed the C-terminal domain of UvrB as a $(His)_6$ tag fusion in *E. coli* and examined the fragment by NMR spectroscopy. The domain contains two stably folded α-helical regions from residues 630 to 648 and from 652 to 670.

2. Materials and methods

2.1. Materials

The C-terminal domain of the UvrB protein has the following sequence (numbers refer to the position in the full-length protein): E^{620}PDNVPMDMSP^{630}KALQQKIHEL^{640}EGLMMQHAQN ^{650}LEFEEAAQIR^{660}DQLHQLRELF^{670}IAAS. The MH_6L tag is at the N-terminus, so that residue numbers in the expressed protein begin at M1 and the natural protein starts at E9 and ends at S63.

The appropriate part of the *uvrB* gene was amplified by PCR using the following primers: 5′-AGCGTAGCGGATCCGGCTGTTTTCCG (introducing a *Bam*HI site after the stop codon of *uvrB*) and 5′-GCGCCCGATTCTCGAGCCGGATAATG (introducing a *Xho*I site at amino acid positions 618 and 619). The *Xho*I-*Bam*HI fragment was ligated into the *Xho*I and *Bam*HI sites of pET3-HisK [5] resulting in pNP118.

The UvrB protein domain was overproduced by transforming BL21:DE3 with pNP118 [6]. A fresh transformant was grown in 50 ml Luria Bertani broth to an A_{600} of 0.5 and inoculated into 2.5 l minimal media (6 g/l K_2HPO_4, 3 g/l KH_2PO_4, 0.5 g/l NaCl, 1 g/l NH_4Cl, 0.2 g/l $MgSO_4$) containing 0.4% glucose, 5 mg/ml thiamine and 80 μg/ml ampicillin. The cells were grown for 12 h at 37°C, induced with isopropylthiogalactoside and grown for a further 4 h before harvesting. For the production of the ^{15}N-labelled protein, the $^{14}NH_4Cl$ in the growth medium was replaced by $[^{15}N]H_4Cl$ and for the $^{13}C/^{15}N$-labelled sample (U-6) $[^{13}C]$glucose was used in addition to $[^{15}N]H_4Cl$.

The cells were resuspended in 15 ml lysis buffer (40 mM Tris, pH 8.0, 10 mM EDTA, 2.4 M sucrose) after which 60 ml buffer B (20 mM potassium phosphate, pH 7.5, 10 mM β-mercaptoethanol) containing 125 mg/ml hen egg lysozyme (Sigma Chemical, Poole, Dorset, UK) was added. The cells were chilled on ice for 30 min followed by centrifugation for 30 min at 35 000 rpm in a Beckman Ti60 rotor. DNA was removed from the lysate by adding NaCl to 1 M and polyethyleneimine P to 0.1% and centrifuging for 20 min at 35 000 rpm using the same rotor. The supernatant was then loaded onto a 10 ml phenyl sepharose column equilibrated with buffer B containing 1 M NaCl and the protein was eluted with a step of buffer B. The fractions containing the UvrB fragment were loaded onto a 1 ml Hi-Trap chelating Ni-column (Pharmacia), washed with buffer B containing 0.5 M NaCl and the protein was eluted with a gradient of 0–0.5 M imidazole in buffer B containing 0.5 M NaCl. Finally, the fractions containing the UvrB fragment were dialysed in either D_2O or 90% H_2O:10% D_2O in 20 mM potassium phosphate, 150 mM NaCl, 0.02% azide buffer pH 7.5 for NMR study and in 20 mM potassium phosphate, 150 mM NaCl buffer pH 7.5 for optical spectroscopy. This procedure resulted in protein preparations at approximately 8–10 mg/ml. As established by SDS-PAGE, the protein samples used for NMR were >95% pure and for optical spectroscopy, they were >98% pure.

*Corresponding author. Fax: (44) (181) 906 4477.
E-mail: alane@nimr.mrc.ac.uk

Abbreviations: CSA, chemical shift anisotropy; HSQC, heteronuclear single quantum coherence; DQF-COSY, double quantum filtered correlation spectroscopy; CD, circular dichroism

PII: S0014-5793(99)00542-6

2.2. Methods

2.2.1. Circular dichroism (CD). CD spectra were recorded on a Jobin-Yvon CD-6 spectropolarimeter, which was fitted with a thermostated cell holder connected to a water bath. Cell path lengths of 1.0, 0.5 and 0.1 mm were used. Spectra were recorded at 20°C, with 0.2 nm steps and an integration time of 1.5 s. The fraction of α-helix was obtained from:

$$\%\alpha = 100(\Delta\varepsilon_{222}-\Delta\varepsilon_R)/(\Delta\varepsilon_H-\Delta\varepsilon_R) \quad (1)$$

where $\Delta\varepsilon_{222}$ is the observed ellipticity at 222 nm, $\Delta\varepsilon_H$ and $\Delta\varepsilon_R$ are values of $\Delta\varepsilon_{222}$ for the fully helical and fully unfolded forms of each sample. The following expressions were used to determine $\Delta\varepsilon_H$ and $\Delta\varepsilon_R$:

$$\Delta\varepsilon_H = (-40000(1-k/n)+100T)/3300 \quad (2)$$

$$\Delta\varepsilon_R = (640-45T)/3300 \quad (3)$$

where T is in °C, n is the number of residues in the chain and $k=2.5$ is a wavelength-dependent constant that corrects for non-hydrogen-bonded carbonyls that do not contribute to $\Delta\varepsilon_H$ [7].

2.2.2. NMR spectroscopy. NMR spectra were recorded at 14.1 T on a Varian Unity spectrometer at 20°C. Spectra in H_2O were recorded using the Watergate method [8] for solvent suppression. NOESY, TOCSY, ROESY and double quantum filtered correlation spectroscopy (DQF-COSY) spectra were recorded on the unlabelled protein using standard methods. The ^{15}N-labelled protein was used for heteronuclear single quantum coherence (HSQC)-NOESY and HSQC-TOCSY experiments [9] and for measurements of the ^{15}N relaxation rate constants (T_1, T_2, $T_{1\rho}$ and NOE). Two dimensional (2D) versions of the HSQC-NOESY experiment were also recorded at different mixing times from 60 to 200 ms for evaluating the secondary structure. The triple resonance experiments CBCA(CO)NH, CBCANH, CC-TOCSY(CO)NH [10,11] were carried out on the ^{15}N, ^{13}C-labelled protein for unambiguous assignment of backbone and side-chain resonances.

Relaxation rate constants were obtained using standard methods with proton decoupling during the variable delay period to suppress chemical shift anisotropy (CSA) dipolar cross-correlation effects [12,13]. Eight delays were used for the T_1 and T_2 experiments. The ^{15}N $T_{1\rho}$ experiment was measured at 14.1 T using a weak CW spin lock ($\gamma B_1 = 2$ kHz) including proton 180° pulses every 2 ms during the spin lock time [12]. The carrier frequency was placed in the centre of the amide nitrogen shift range. Peak volumes were fitted to a single exponential decay function:

$$I(\tau) = I(0)\exp(-R\tau) \quad (4)$$

where $I(\tau)$ is the intensity at delay time τ, $I(0)$ the intensity at $\tau=0$ and R is the relaxation rate constant. Offset effects in the $T_{1\rho}$ experiment were corrected according to the projection relations [14]:

$$R_{1\rho}\ (\text{obs}) = \sin^2\phi\, R_1 + \cos^2\phi\, R_2 \quad (5)$$

where ϕ is the tilt angle of the effective spin lock field. As the maximum offset was <500 Hz, the corrections are small. The NOE experiments were carried out with a relaxation delay of 4.4 s, which is 4–6 times the ^{15}N T_1 values.

The secondary structure was assigned using the chemical shift index (Cα and Hα) [15,16] and the sequential NH(i)−NH(i+1) and CαH(i)−CαH(i+3, 4) NOEs.

Backbone dynamics were determined from the heteronuclear relaxation data by spectral density mapping [12,17]. The expressions for R_{12}^D and R_{12}^{CSA} were as defined [12]. The magnitude of the CSA was fixed at −160 ppm and the N-H bond length of 1.02 Å was assumed [12]. Spectral densities at zero, ω_H and ω_N were calculated as:

$$J(\omega_H) = (\text{NOE}-1)\gamma_N r^6/(6.61\gamma_H\alpha R_1) \quad (6)$$

$$J(0) = R_2-0.5R_1-3(\alpha/r^6)J(\omega_H)/(\alpha/r^6(2+3J(\omega_H)) + 88.88\times10^{-6}\Delta\sigma^2\omega_N^2) \quad (7)$$

$$J(\omega_N) = (R_1-8.21\alpha/r^6(J(\omega_H))/(3\alpha/r^6+133.333\times10^{-6}\Delta\sigma^2\omega_N^2) \quad (8)$$

$$J(\omega) = \tau/(1+\omega^2\tau^2)) \quad (9)$$

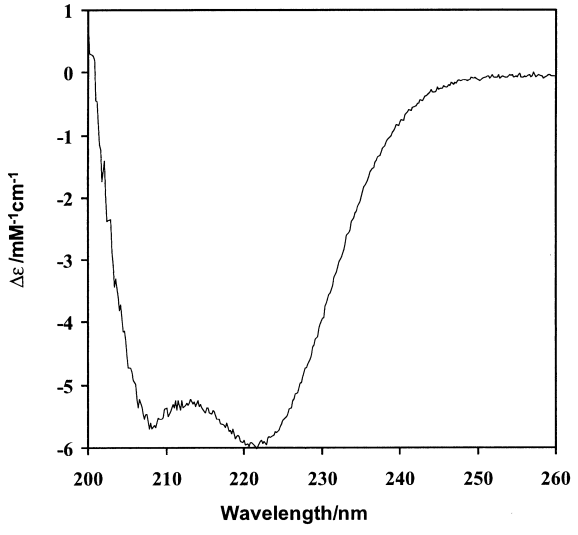

Fig. 1. CD spectrum of the UvrB C-terminal domain. The spectrum was recorded at 20°C as described in Section 2.2.

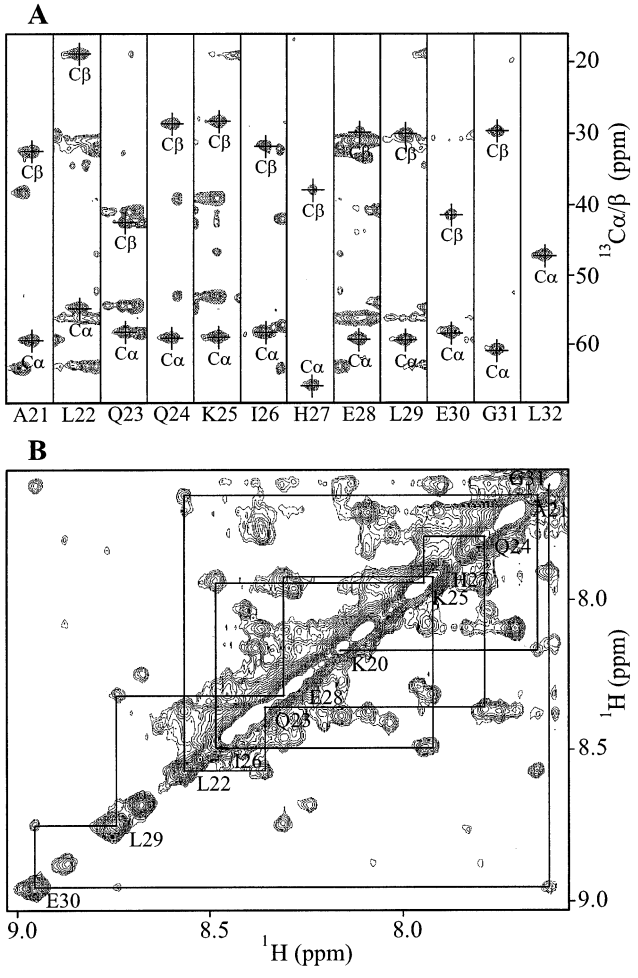

Fig. 2. NMR assignment of backbone atoms in the UvrB C-terminal domain. Assignments were made using heteronuclear NMR spectroscopy. A: Strips from the CBCA(CO)NH triple resonance experiment recorded at 14.1 T and 20°C. Residues A21–L32 are shown. B: NH-NH NOEs in ^{15}N-edited HSQC-NOESY. The spectrum was recorded as described in Section 2.2, with a mixing time of 100 ms. Lines show sequential NH-NH NOE connectivities from K20 to G31 in the first helical segment.

Table 1
NMR assignments of the UvrB C-terminal domain

Residue	H_N	N	Cα	Hα	Cβ	Hβ	Cγ	Hγ	Cδ	Hδ	Other
E9	8.38	123.26	54.28	4.53	29.68	2.04, 1.86	36.06	2.27			
P10			63.67	4.34	32.13	1.91, 2.25	27.51	1.96, 2.00	50.63	3.70, 3.75	
D11	8.42	119.23	54.54	4.53	41.01	2.59, 2.66					
N12	8.28	118.40	53.20	4.71	39.20	2.71, 2.78					112.30Nδ 6.90, 7.62Hδ
V13	7.96	121.64	60.05	4.34	32.66	2.06	21.22, 20.69	0.93, 0.89			
P14			63.14	4.38	32.24	1.91, 2.25	27.53	1.93, 2.02	50.95	3.83, 3.63	
M15	8.45	120.80	56.04	4.33	33.30	2.00	31.98	2.53, 2.55			17.06Cε 2.06Hε
D16	8.27	121.40	54.15	4.53	40.98	2.64, 2.70					
M17	8.16	121.27	54.58	4.53	32.33	1.89	32.59	2.61, 2.46			17.28Cε 2.03Hε
S18	8.39	118.64	56.92	4.66	62.97	4.05, 4.24					
P19			66.39	4.25	31.79	2.08, 2.33	27.73	1.96, 1.99	50.03	3.48, 3.56	
P19[a]						1.96, 2.23			50.32	3.91, 3.94	
K20	8.17	116.42	59.40	4.09	32.44	1.74, 1.88	25.05	1.40, 1.50	29.20	1.68	42.10Cε 2.98Hε
A21	7.66	123.27	54.83	4.18	18.54	1.47					
L22	8.57	120.93	58.17	4.06	42.56	1.94	24.97	1.50	24.61, 24.31	0.92, 0.84	
Q23	8.36	117.87	59.13	3.59	28.55	2.06	34.08	2.09, 2.14			111.31Nε 6.81, 6.91Hε
Q24	7.80	118.73	59.00	4.10	28.23	2.12, 2.21	33.80	2.42, 2.51			111.85Nε 6.88, 7.71Hε
K25	7.95	121.52	58.28	4.18	31.64	2.01	24.70	1.48	28.35	1.74	41.88Cε 2.84Hε
I26	8.49	119.98	65.88	3.47	38.04	1.74	26.84, 16.66	1.09, 0.77	13.54	0.57	
H27	7.93	117.71	59.22	4.47	29.78	3.24					
E28	8.32	121.00	59.36	3.99	29.89	2.22, 2.28	36.24	2.18, 2.48			
L29	8.73	120.92	58.31	4.12	41.48	2.04, 1.37	24.68	1.26	25.70, 22.62	0.97, 0.91	
E30	8.94	120.54	60.83	3.85	29.70	1.98	38.08	2.17, 2.62			
G31	7.63	105.21	47.27	3.83, 3.91							
L32	7.91	124.37	57.82	4.04	42.63	1.67, 1.84	24.42	1.21	23.83, 23.43	0.86, 0.88	
M33	9.04	120.04	60.82	3.75	33.49	2.00	30.91	2.49, 2.64			17.30Cε 2.26Hε
M34	7.78	114.88	57.41	4.44	30.95	2.22	32.13	2.81			16.72Cε 2.15Hε
Q35	8.04	122.27	59.10	4.00	28.66	2.06	33.91	2.14, 2.25			111.42Nε 6.73, 7.28Hε
H36	8.40	117.20	59.70	4.46	27.92	2.97, 3.00					
A37	8.46	121.79	55.85	3.64	18.65	1.69					
Q38	8.31	118.64	58.50	3.99	28.35	2.12, 2.21	34.09	2.47			111.03Nε 6.81, 7.45Hε
N39	7.26	115.82	52.70	4.73	38.90	2.55, 2.94					112.43Nδ 6.86, 7.46Hδ
L40	7.62	113.93	55.44	4.00	37.80	2.11	25.69	0.90	25.54, 22.83	0.84, 0.91	
E41	8.14	123.72	53.49	4.46	26.24	2.15	35.21	2.11, 2.19			
F42	6.91	118.41	60.26	3.96	39.52	3.03, 3.23			131.49	7.44	132.82Cε 7.66Hε 129.95Cζ 7.01Hζ
E43	10.4	124.03	61.51	3.93	26.99	1.70	37.49	2.24, 2.66			
E44	8.75	122.04	59.99	3.72	26.97	1.86	37.22	1.94, 2.01			
A45	7.84	120.45	55.68	3.64	15.67	0.46					
A46	8.12	120.11	55.55	4.26	17.99	1.59					
Q47	7.26	116.13	58.99	4.11	28.35	2.15	33.82	2.39, 2.52			111.21Nε 6.81, 7.39Hε
I48	7.81	119.94	64.24	3.80	37.21	1.82	28.93, 20.92	1.14, 1.14	12.69	0.88	
R49	8.87	122.80	59.85	4.10	29.81	2.08	25.76	2.00	43.74	3.38, 3.61	109.79Nε 6.74Hε
D50	8.09	119.92	57.56	4.61	39.38	2.81, 2.87					
Q51	7.94	123.10	59.25	4.19	28.93	2.32	34.08	2.32, 2.59			109.06Nε 6.76, 7.28Hε
L52	9.16	121.91	58.45	3.97	42.62	2.09	26.93	1.10	26.35, 26.06	1.02, 0.82	
H53	8.24	118.11	59.84	4.39	30.44	3.35					
Q54	7.44	116.83	58.72	4.13	28.66	2.27	34.06	2.43, 2.61			111.23Nε 6.91, 7.51Hε
L55	8.25	120.08	58.11	4.11	42.20	1.50	26.59	1.82	26.66, 23.25	0.86, 0.85	
R56	8.67	118.23	60.42	3.98	29.72	1.95	29.17	1.91	43.47	3.19	109.69Nε 7.36Hε
E57	7.56	117.94	59.18	4.05	29.63	2.10	36.58	2.15, 2.31			
L58	7.76	120.14	57.30	4.12	42.07	1.99	25.15	1.51	25.46, 23.08	0.91, 0.87	
F59	8.37	119.79	60.50	4.22	39.68	3.03, 3.23			131.58	7.20	131.61Cε 7.32Hε 130.08Cζ 7.25Hζ
I60	8.09	120.70	63.41	3.70	38.29	1.91	28.62, 17.35	1.27, 0.91	13.21	0.87	
A61	7.72	123.33	53.33	4.21	18.80	1.45					
A62	7.73	121.50	52.38	4.35	19.53	1.38					
S63	7.53	120.45	60.55	4.14	64.99	3.67, 3.75					

[a]The second conformation of H^{β}, C^{δ}, H^{δ} of P19.

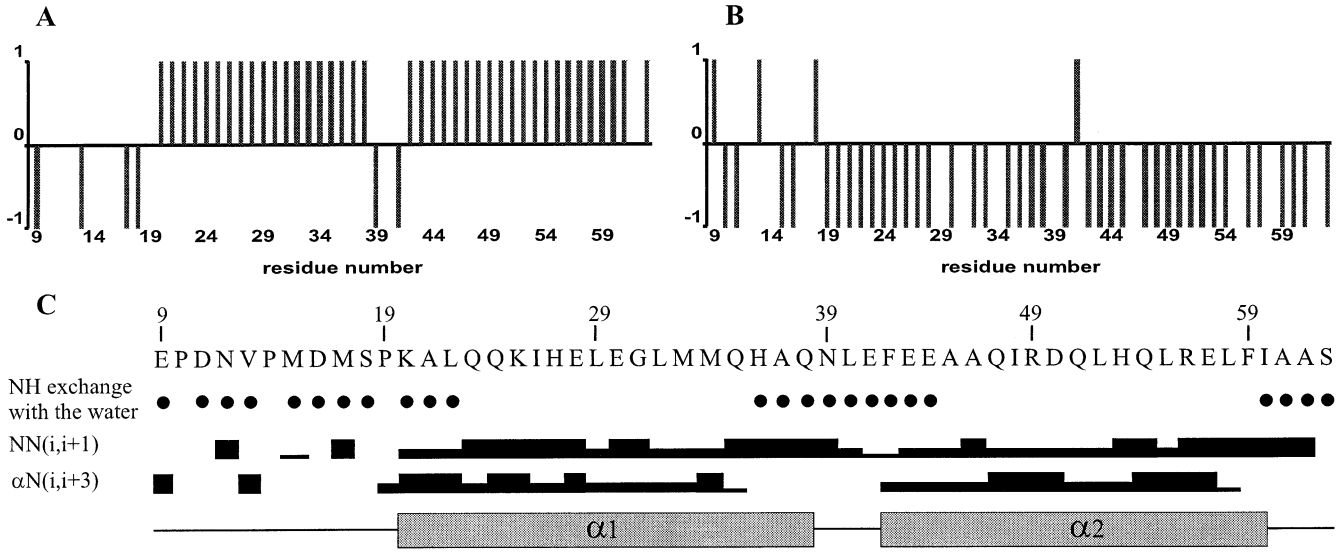

Fig. 3. Secondary structure of the UvrB C-terminal domain. Secondary structure elements were defined from the Cα (A) and Hα (B) chemical shift indices, NOE intensities (C) and NH exchange rates as described in the text.

where τ is the correlation time and α is a constant. The spectral densities at ω_H, $\omega_H \pm \omega_N$ can be combined, such that at $B_0 = 14.1$ T $J(\omega_H+\omega_N) = 1.235J(\omega_H)$ and $J(\omega_H-\omega_N) = 0.826J(\omega_H)$.

3. Results

3.1. CD spectroscopy

The far UV CD spectrum (200–260 nm) is typical of an α-helix with minima at 208 and 222 nm. Fig. 1 shows a CD spectrum of the UvrB fragment recorded at a concentration of 350 μg/ml. From the ellipticity at 222 nm and using Eq. 1, we estimate a helical content of at least 53%.

3.2. NMR spectroscopy

Fig. 2A shows strips from the CBCA(CO)NH experiment which provides sequential connectivities along the entire protein. Fig. 2B shows the NH-NH sequential connectivities in ^{15}N-edited HSQC-NOESY. Essentially complete connectivities could be followed in either 2D or three dimensional (3D) experiments from residues 20 to 62, which are characteristic of α-helices. All of the backbone atoms could be unambiguously assigned (Table 1). Side-chain assignments were obtained using the CC-TOCSY(CO)NH experiment. Correlation with protons was obtained with the ^{13}C HSQC experiment. A high resolution experiment of this kind (i.e. in which the C-C couplings are resolved) was helpful for distinguishing between the Cα and Cβ of serine and the ends of side-chains or Pro δ. Additional checks were provided by the TOCSY-HSQC and NOESY experiments. Side-chain amide protons were identified in the HSQC experiment and connected to Cβ+Cα or Cγ+Cβ in the CBCA(CO)NH experiment.

In NOESY experiments in H_2O, a group of NH resonating near 8.3 ppm showed exchange peaks with the water, indicating an exchange time in the order of the mixing time of the experiment (60–100 ms). Other resonances, corresponding to residues 23–35 and 45–59 showed no exchange on the same time scale. The group of resonances that exchange rapidly with solvent and have NH shifts near 8.3 ppm is likely to be unstructured and not involved in hydrogen binding within the protein.

Fig. 3 shows the deviations of the chemical shifts of Cα and Hα from their random coil values, the d_{NN} and $d_{\alpha Ni,\,i+3}$, intensities along the sequence and the presence of slow and fast exchanging amide protons. These data show the presence of two helical segments from residues 20 to 38 and from 42 to 60, with a break comprising residues 39–41. Residues 9–19 appear disordered. This is not surprising as residues 10, 14 and 19 are proline. Thus, according to the NMR data, the

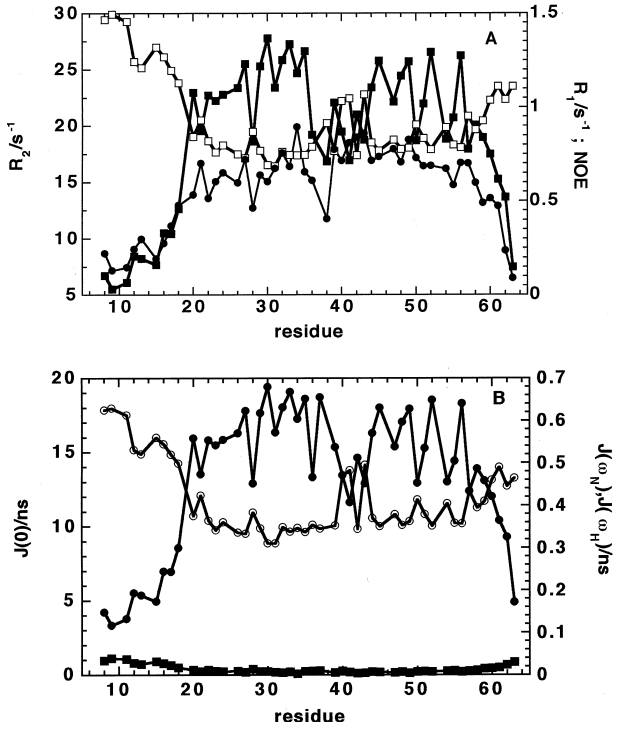

Fig. 4. ^{15}N relaxation in the UvrB C-terminal domain. ^{15}N relaxation measurements were made at 20°C and 14.1 T as described in Section 2.2. A: (■) R_2, (□) R_1 and (●) NOE along the sequence. B: Spectral densities at (●) 0, (○) 60 and (■) 600 MHz.

protein is about 65% helical, which is consistent with the CD result (see above).

For a protein of 63 residues, the first few of which are disordered, the ^{15}N NMR line-widths would be expected to be narrow (circa 3–4 Hz). However, in a high resolution ^{15}N-HSQC experiment, the line-widths of the amide N for the structured residues were circa twice the values expected for a monomer of 7.5 kDa, suggesting that the protein is not primarily a monomer in solution. Fig. 4A shows the measured values of R_2, R_1 and NOE along the sequence. The values of R_2 are small up to residue 19, reach an average of circa 22/s for residues 20–60 and drop again for the last three residues. Similarly, R_1 is smaller between residues 20–60 than in the N-terminal and C-terminal regions and the NOE is larger in the core (residues 20–60) than at the termini. This correlates well with the secondary structure (see above). The value of $R_{1\rho}$ determined on the same sample was within 10% of the value of R_2 (not shown), showing that R_2 does not contain a large contribution from chemical exchange processes on the ms–μs time-scale. Fig. 4B shows the value of $J(0)$ obtained from the spectral density mapping approach [12,17]. $J(0)$ is large for residues 20–60, but is circa 3-fold smaller for the residues 9–19 and the last three residues. The spectral densities at ω_N (60 MHz) and ω_H (600 MHz) showed the opposite trend, with low values for residues 20–60 and values that increase gradually from the low values in the core to higher (5–6-fold) values at the chain termini. The spectral densities at all three frequencies for residues 20–60 are as expected for a relatively rigid molecule. The values of the spectral densities near the chain termini cannot be described with a single correlation time and require a faster motion at zero frequency and additional motions near ω_N and ω_H.

4. Discussion

The chemical shift, NOESY and CD data show that the protein consists of two unstructured segments (residues 9–19 and 61–63) and between them, two regions (residues 20–38 and 42–60) in α-helical conformations. The presence of a structured region flanked by dynamically unstructured segments is confirmed by the ^{15}N relaxation (Fig. 4). The observed $J(0)$ are large for a monomer of $M = 7.5$ kDa (τ circa 3–4 ns). The relaxation data are consistent with either an anisotropic dimer [18] or a spherical tetramer.

As this domain is involved in heterodimerisation with a homologous domain within UvrC, there should be a tendency to self-dimerise. Comparison of the UvrB proteins from different bacteria shows that the 'hinge' between the conserved C-terminal domain and the remainder of the protein varies substantially both in sequence and in length (16–64 residues [2]). Moreover, this region in *E. coli* UvrB is very sensitive to a wide range of proteases (resulting in UvrB*). However, there is no tendency of intact UvrB to dimerise. This may be in part because the free domains have a relatively low affinity for one another and therefore do not dimerise at the low concentrations used in previous work. It is also possible that the remainder of the protein in native UvrB interferes with self-dimerisation.

Two simple models of self-dimerisation can be proposed. One is the formation of a helical coiled-coil [3], the other is dimerisation of a two-helical bundle to form a four-helix bundle. At present, we cannot distinguish between these possibilities. However, this domain has a high homology to a two-helix bundle present in a de novo synthesised peptide [19].

For the UvrABC system to function, the effective homodimerisation must be much weaker than heterodimerisation with UvrC, at least in the presence of DNA. We are currently trying to estimate the homodimerisation constant and the structure from the NOEs. In order to determine the mode of dimerisation, it will be necessary to break the symmetry of the system, which should be achievable by making a mixture of labelled with unlabelled protein [20].

Acknowledgements: This work was supported by the MRC and an EU Structural Biology Framework IV Programme grant. NMR spectra were recorded at the MRC Biomedical NMR Centre, Mill Hill. We are grateful to Dr. T. A. Frenkiel for assistance with NMR experiments, and Dr. J. Saldanha for analysing sequence alignments.

References

[1] Sancar, A. (1998) Ann. Rev. Biochem. 65, 43–63.
[2] Goosen, N., Moolenaar, G.F., Visse, R. and van de Putte, P. (1998) In: Nucleic Acids and Molecular Biology 12 (Eckstein, F. and Lilley, D.M.F., Eds.), pp. 103–123, Springer-Verlag, Berlin, Germany.
[3] Moolenaar, G.F., Franken, K.L.M.C., Dijkstra, D.M., Thomas-Oates, J.E., Visse, R., van de Putte, P. and Goosen, N. (1995) J. Biol. Chem. 270, 30508–30515.
[4] Moolenaar, G.F., Franken, K.L.M.C., van de Putte, P. and Goosen, N. (1998) Mutat. Res. 385, 195–203.
[5] Chen, B.P.C. and Hai, T. (1994) Gene 139, 73–75.
[6] Studier, F.W., Rosenberg, A.H., Dunn, J.J. and Dubendorff, J.W. (1990) Methods Enzymol. 185, 60–89.
[7] Scholtz, J.M., Quian, H., York, E.J., Stewart, J.M. and Baldwin, R. (1991) Biopolymers 31, 1463–1470.
[8] Piotto, M., Saudek, V. and Sklenar, V. (1992) J. Biomol. Struct. 2, 661–665.
[9] Bodenhausen, G. and Ruben, D.J. (1980) Chem. Phys. Lett. 69, 185–189.
[10] Cavanagh, J., Fairbrother, W.J., Palmer, A.G. III, Skelton, N.J. (1996) Protein NMR Spectroscopy. Principles and Practice. Chapter 7, Academic Press, San Diego, CA, USA.
[11] Grzesiek, S., Anglister, J. and Bax, A. (1993) J. Magn. Reson. 101B, 114–119.
[12] Peng, J.W. and Wagner, G. (1992) J. Magn. Reson. 98, 308–332.
[13] Kay, L.E., Nicholson, L.K., Delaglio, F., Bax, A. and Torchia, D.A. (1992) J. Magn. Reson. 97, 359–375.
[14] Davis, D.G., Perlman, M.E. and London, R.E. (1994) J. Magn. Reson. B104, 266–275.
[15] Wishart, D.S., Sykes, B.D. and Richards, F.M. (1992) Biochemistry 31, 1647–1651.
[16] Wishart, D.S. and Sykes, B.D. (1994) J. Biomol. NMR 4, 171–180.
[17] Lefèvre, J.-F., Dayie, K.T., Peng, J.W. and Wagner, G. (1996) Biochemistry 35, 2674–2686.
[18] Schurr, J.M., Babcock, H.P. and Fujimoto, B.S. (1994) J. Magn. Reson. B105, 211–224.
[19] Schafmeister, C.E., LaPorte, S.L., Miercke, L.J.W. and Stroud, R.M. (1997) Nat. Struct. Biol. 4, 1039–1046.
[20] Lee, W.T., Harvey, T.S., Yin, Y., Yau, P., Litchfield, D. and Arrowsmith, C.H. (1994) Nat. Struct. Biol. 1, 877–890.